Low-Complexity EM-based Joint acquisition of the Carrier Frequency Offset and IQ imbalance

François Horlin, André Bourdoux, Eduardo Lopez-Estraviz, and

Liesbet Van der Perre

Interuniversity Micro-Electronic Center, IMEC

Wireless Research

Kapeldreef 75, B-3001 Leuven, Belgium

Email: *fhorlin@ulb.ac.be*

Abstract

New air interfaces are currently being developed to meet the high spectral efficiency requirements of the emerging wireless communication systems. In this context, OFDM is considered as a promising air interface candidate for both indoor and outdoor communications. Besides spectral efficiency and power consumption, the production cost of the transceiver should also be optimized. Direct-conversion radio frequency receivers are appealing because they avoid costly intermediate frequency hardware. However, they imply analog IQ separation, introducing a phase and amplitude mismatch between the I and Q branches. A communication system based on OFDM is sensitive to synchronization errors, such as CFO, and to front-end non-idealities, such as IQ imbalance. The goal of this paper is to use the iterative EM algorithm to acquire jointly the CFO and the IQ imbalance. The solution relies on a repetitive preamble and does not require the knowledge of the propagation channel. Based on a second order approximation of the likelihood function, the complexity of the EM algorithm is significantly reduced. The algorithm is shown to perform extremely well: the estimates of the CFO and of the IQ imbalance converge to their ML estimate after less than 3 iterations. While the CFO estimate is robust against variations of the SNR, the IQ imbalance estimate accuracy is reduced at values of the SNR below 10 dB and above 35 dB.

Keywords

Carrier Frequency Offset, IQ imbalance, Synchronization, Acquisition, Expectation-Maximization

I. INTRODUCTION

Orthogonal frequency-division multiplexing (OFDM) is a popular technology to increase the spectral and power efficiency of the new wireless communication systems. While OFDM is already integrated in the wireless local area networks (WLAN) [1], its use is also foreseen in the emerging cellular systems [2]. The main advantage of OFDM comes from the possible equalization of the multipath propagation channel at a low complexity in the frequency domain.

On the other hand, integrated direct-conversion analog front-ends are envisaged to replace the classical super-heterodyne structure because they avoid costly intermediate frequency (IF) hardware [3]. Since the IQ demodulation is directly performed in the analog domain (rather than a first down-conversion to an intermediate frequency in the analog domain followed by an IQ demodulation in the digital domain), the system suffers from a phase and amplitude mismatch between the I and Q branches.

Though OFDM is robust against the interference caused by the multipath propagation, it is sensitive to the system non-idealities that destroy the orthogonality between the carriers. Especially, the carrier frequency offset (CFO), caused by the local oscillators at the transmitter and

receiver, and the IQ imbalance, caused by the use of direct-conversion analog front-ends, are destructive [4]. It has been recently shown that those effects can be advantageously compensated digitally [5]. Therefore, it is particularly important to develop efficient schemes to estimate the CFO and the IQ imbalance.

Schmidl and Cox have shown that a preamble composed of two identical parts could be used to estimate efficiently the CFO irrespective of the multipath channel [6]. The maximum likelihood (ML) estimate of the CFO consists in assessing the received signal phase drift due to the CFO by correlating the two parts of the received signal with each other. Because the IQ imbalance degrades the estimation of the CFO (and reciprocally), the two effects need to be estimated together. Papers [7] and [8] introduce two different estimators of the CFO in the presence of IQ imbalance. The estimator proposed in [7] relies on a specifically designed pilot symbol in the frequency domain consisting of only one loaded carrier. The CFO and IQ imbalance are estimated iteratively to minimize the energy that they cause on the unloaded carriers. On the contrary, [8] defines a measure of the CFO whose expectation is independent of the IQ imbalance, and averages it over multiple short training sequences (compatible with the time-domain periodic training sequence imposed by the IEEE 802.11a WLAN standard). On the other hand, [9] proposes an estimator of the IQ imbalance in the presence of CFO. It exploits the fact that IQ imbalance destroys the smoothness of the propagation channels in the frequency domain and deduces the IQ imbalance by observing the abrupt changes in the estimated frequency response. Interestingly, [10] proposes an integrated structure to compensate for the CFO and for frequency-dependent IQ imbalance. Again, the estimator relies on a specifically designed training sequence consisting of multiple identical blocks, where the even blocks are rotated by a common phase. Finally, we have also proposed a new preamble structure to facilitate the joint CFO and IQ imbalance estimation taking the very strict specifications of the emerging 4G wireless systems into account [11].

In this paper, we make use of the expectation-maximization (EM) algorithm [12] to estimate iteratively the CFO and IQ imbalance. We rely on the periodic structure of the preamble to make the estimate independent of the channel knowledge (the preamble can be any sequence repeated one time). In order to achieve a tractable solution, the ML function is simplified making a second order approximation. The paper is organized as follows. The system is described in Section II, yielding the reference vector model. In Section III, the likelihood function is computed

and simplified. The EM algorithm is derived from the expression of the likelihood function in Section IV. The expressions are modified in Section V until an implementable form of the EM algorithm is obtained. Finally, Section VI assesses the performance of the proposed solution and Section VII concludes the paper.

In the sequel, the operator $\otimes$ denotes the convolution between two signals. We use single- and double-underlined letters for the vectors and matrices respectively. The operators $(.)^*$, $(.)^T$ and $(.)^H$ denote respectively the complex conjugate, transpose and hermitian of a vector or a matrix.

II. System model

A. Functional description

A simplified model of the system is illustrated in Figure 1. The transmitted preamble $p[n]$ consists of a cyclic prefix of size L at least equal to the channel impulse response length followed by a complex sequence $a[n]$ of length $Q >> L$ repeated one time ($a[n]$ is different from 0 for $n = 0, \cdots, Q-1$). The cyclic prefix is formed with the last samples of the sequence $a[n]$. The preamble sequence $p[n]$ is defined mathematically as:

$$p[n] := \begin{cases} a[mod(n,Q)] & \text{if} \quad n = -L, \cdots, 2Q-1, \\ 0 & \text{else}\,. \end{cases} \tag{1}$$

The sample duration is denoted by T. The baseband signal is up-converted to the carrier frequency ω_0, after low-pass filtering by $\psi_T(t)$ in order to remove the out-of-band components. The resulting signal, $s_{RF}(t)$, is transmitted through a frequency selective channel $h_{RF}(t)$. Additive white Gaussian noise (AWGN), $w_{RF}(t)$, of one-sided power spectral density equal to N_0, is added in the first amplifier stages of the receiver front-end. The radio frequency (RF) received signal, $r_{RF}(t)$, is finally down-converted to the baseband domain for complex operation, low-pass filtered with the filter $\psi_R(t)$ in order to avoid aliasing, sampled at a rate $1/T$ and serial-to-parallel converted to form the received vector $\underline{Z}$. Because the preamble is repetitive, the received vector should be repetitive as well. However, this property is destructed by the system non-idealities (CFO and IQ imbalance).

B. Non-idealities

Due to the use of different local oscillators at the transmitter and at the receiver, the down-conversion to the baseband domain is operated with a phase shift ϕ_0 and with a frequency shift

$\Delta\omega$ (CFO). On the other hand, IQ imbalance caused by the use of different elements on the I and Q branches, is modeled by a difference in amplitude ϵ and phase $\Delta\phi$ between the two branches. If $r(t) := r_r(t) - jr_i(t)$ is the baseband representation of the RF received signal $r_{RF}(t)$, we have that:

$$r_{RF}(t) \;=\; r_r(t)\cos(\omega_0 t) \;+\; r_i(t)\sin(\omega_0 t)\,. \tag{2}$$

Taking the CFO and IQ imbalance into account, the baseband component of the signal on the I branch after multiplication by the cosine is:

$$y_r(t) \;=\; +\,r_r(t)\,(1+\epsilon)\,\cos(\Delta\phi + \Delta\omega t + \phi_0) \;-\; r_i(t)\,(1+\epsilon)\,\sin(\Delta\phi + \Delta\omega t + \phi_0)\,, \tag{3}$$

and the baseband component of the signal on the Q branch after multiplication by the sine is:

$$y_i(t) \;=\; -\,r_r(t)\,(1-\epsilon)\,\sin(\Delta\phi - \Delta\omega t - \phi_0) \;+\; r_i(t)\,(1-\epsilon)\,\cos(\Delta\phi - \Delta\omega t - \phi_0)\,. \tag{4}$$

We are not interested in the high frequency components resulting from the multiplication with the cosine and sine because they will be later filtered out by the low-pass filter $\psi_R(t)$. By defining $y(t) := y_r(t) - jy_i(t)$, we get that:

$$y(t) \;=\; \alpha\, e^{-j(\Delta\omega t+\phi_0)}\, r(t) \;+\; \beta\, e^{j(\Delta\omega t+\phi_0)}\, r^*(t) \tag{5}$$

in which:

$$\alpha \;:=\; \cos(\Delta\phi) - j\epsilon\sin(\Delta\phi) \tag{6}$$

$$\beta \;:=\; \epsilon\cos(\Delta\phi) + j\sin(\Delta\phi)\,. \tag{7}$$

The parameters α and β express the impact of the IQ imbalance on the received signal ($\alpha = 1$ and $\beta = 0$ when the two paths are exactly the same). The CFO leads to a frequency shift of the two components of the baseband received signal, as shown in (5).

After low-pass filtering, the received signal is given by:

$$z(t) \;=\; y(t) \otimes \psi_R(t) \tag{8}$$

$$\;=\; \alpha\, e^{-j(\Delta\omega t+\phi_0)}\,(r(t) \otimes \psi_R(t) e^{j\Delta\omega t}) \;+\; \beta\, e^{j(\Delta\omega t+\phi_0)}\,(r(t) \otimes \psi_R(t) e^{j\Delta\omega t})^*\,. \tag{9}$$

It is sampled at the rate $1/T$ to get the received sequence $z[n] := z(t = nT)$.

C. Input/Output relationship

Based on (9), the received sequence can be expressed as a function of the transmitted preamble as:

$$z[n] \;=\; \alpha\, e^{-j(\Delta\omega nT+\phi_0)}\,(p[n]\otimes g[n]) \;+\; \beta\, e^{j(\Delta\omega nT+\phi_0)}\,(p[n]\otimes g[n])^* \;+\; v[n] \qquad (10)$$

in which $g[n]$ is the digital equivalent impulse response defined as:

$$g[n] := (\psi_T(t)\otimes h(t)\otimes \psi_R(t)\, e^{j\Delta\omega t})_{|t=NT}\,. \qquad (11)$$

In the last expression, $h(t)$ is the baseband representation of $h_{RF}(t)$. We assume that $g[n]$ has a finite length $L_g \leq L$. The noise sequence, $v[n]$, is obtained by observing $w_{RF}(t)$ at the output of the receiver analog front-end. Assuming that the filter $\psi_R(t)$ is a perfect low-pass filter of bandwidth $1/T$, the noise samples are independent of variance $\sigma_v^2 = 2N_0/T\dot{(}1+\epsilon^2) \simeq 2N_0/T$.

D. Vector model

After serial-to-parallel conversion, the received vector $\underline{Z}$ can be decomposed into four parts (see Figure 1): $\underline{Z}_{cp}$ of size L corresponding to the cyclic prefix, $\underline{Z}_0$ and $\underline{Z}_1$ of size Q corresponding to the repeated parts of the preamble, and $\bar{\underline{Z}}$ of size L_g-1 caused by the convolution of the last samples of the preamble with the channel impulse response. By focusing on the parts $\underline{Z}_0$ and $\underline{Z}_1$ of the received vector given by:

$$\underline{Z}_0 \;:=\; [z[0]\cdots z[Q-1]]^T \qquad (12)$$

$$\underline{Z}_1 \;:=\; [z[Q]\cdots z[2Q-1]]^T\,, \qquad (13)$$

and by defining the noise vectors as:

$$\underline{V}_0 \;:=\; [v[0]\cdots v[Q-1]]^T \qquad (14)$$

$$\underline{V}_1 \;:=\; [v[Q]\cdots v[2Q-1]]^T\,, \qquad (15)$$

we get finally:

$$\underline{Z}_0 \;=\; \underline{X} \;+\; \bar{\beta}\,\underline{X}^* \;+\; \underline{V}_0 \qquad (16)$$

$$\underline{Z}_1 \;=\; e^{-j\phi}\,\underline{X} \;+\; \bar{\beta}\, e^{j\phi}\,\underline{X}^* \;+\; \underline{V}_1 \qquad (17)$$

in which $\underline{X} := [x[0] \cdots x[Q-1]]^T$ with $x[n] := \alpha\, e^{-j(\Delta\omega nT+\phi_0)}\,(p[n] \otimes g[n])$ is the reference received vector, $\phi := \Delta\omega QT$ is the phase difference between the two received signal parts due to the CFO, and $\bar{\beta} := \beta/\alpha^*$ is the modified IQ imbalance. In the absence of IQ imbalance ($\bar{\beta} = 0$), the CFO is usually estimated by observing the phase difference ϕ between $\underline{Z}_0$ and $\underline{Z}_1$ [6].

The ultimate goal is to exploit the redundancy in the received signal in order to build an estimate of the CFO and IQ imbalance independent of the propagation channel. It is therefore interesting to express the second part of the received signal $\underline{Z}_1$ as a function of the first part $\underline{Z}_0$. Based on (16), it is clear that:

$$\underline{X} \;=\; \frac{\underline{Z}_0 \,-\, \bar{\beta}\,\underline{Z}_0^*}{1 \,-\, |\bar{\beta}|^2} \;-\; \frac{\underline{V}_0 \,-\, \bar{\beta}\,\underline{V}_0^*}{1 \,-\, |\bar{\beta}|^2}\,. \tag{18}$$

By introducing (18) in (17), we get:

$$\underline{Z}_1 \;=\; \lambda(\phi,\bar{\beta})\,\underline{Z}_0 \;+\; \mu(\phi,\bar{\beta})\,\underline{Z}_0^* \;+\; \underline{N} \tag{19}$$

in which the parameters $\lambda(\phi,\bar{\beta})$ and $\mu(\phi,\bar{\beta})$ are defined as:

$$\lambda(\phi,\bar{\beta}) \;:=\; \cos\phi \;-\; j\,\sin\phi\,\frac{1 \,+\, |\bar{\beta}|^2}{1 \,-\, |\bar{\beta}|^2} \tag{20}$$

$$\mu(\phi,\bar{\beta}) \;:=\; 2\,j\,\sin\phi\,\frac{\bar{\beta}}{1 \,-\, |\bar{\beta}|^2}\,, \tag{21}$$

and the noise vector $\underline{N}$ is given by:

$$\underline{N} \;:=\; -\lambda(\phi,\bar{\beta})\,\underline{V}_0 \;-\; \mu(\phi,\bar{\beta})\,\underline{V}_0^* \;+\; \underline{V}_1\,. \tag{22}$$

It is shown in appendix that the noise vector is formed with Gaussian independent elements of zero mean and of variance equal to:

$$\sigma_n^2(\phi,\bar{\beta}) \;=\; \sigma_v^2\,\left(2 \,-\, |\bar{\beta}|^2 \,+\, 8\,(\sin\phi)^2\,\frac{|\bar{\beta}|^2}{1 \,-\, |\bar{\beta}|^2}\right)\,. \tag{23}$$

III. Likelihood function

The ML estimate of the CFO and IQ imbalance is given by the set of parameters ϕ and $\bar{\beta}$ that maximizes the function:

$$\Lambda(\phi,\bar{\beta}) \;:=\; \log p\left(\underline{Z}_1 | \underline{Z}_0, \phi, \bar{\beta}\right) \tag{24}$$

$$\begin{aligned} &=\; -\,\frac{Q}{2}\log\left(2\pi\sigma_n^2(\phi,\bar{\beta})\right) \\ &\quad -\,\frac{1}{2\sigma_n^2(\phi,\bar{\beta})}\cdot\left(\underline{Z}_1 - \lambda(\phi,\bar{\beta})\underline{Z}_0 - \mu(\phi,\bar{\beta})\underline{Z}_0^*\right)^H\cdot\left(\underline{Z}_1 - \lambda(\phi,\bar{\beta})\underline{Z}_0 - \mu(\phi,\bar{\beta})\underline{Z}_0^*\right) \end{aligned} \tag{25}$$

where the last equality (25) has been obtained based on (19) in which the noise vector has a Gaussian distribution.

Introducing the terms (20), (21) and (23) in the likelihood function (25) does not lead to a tractable function. For reasonable values of the signal-to-noise ratio (SNR), the first term is negligible compared to the second term (σ_v^2 is small). On the other hand, because the IQ mismatch parameter $\bar{\beta}$ is small for actual analog front-ends ($\bar{\beta} << 1$), we can approximate the likelihood function by making a second order approximation. The terms (20), (21) and (23) are approximately equal to:

$$\lambda(\phi,\bar{\beta}) \;\approx\; e^{-j\,\phi} \;-\; 2\,j\;\sin\phi\,|\bar{\beta}|^2 \tag{26}$$

$$\mu(\phi,\bar{\beta}) \;\approx\; 2\,j\;\sin\phi\,\bar{\beta} \tag{27}$$

$$\sigma_n^2(\phi,\bar{\beta}) \;\approx\; 2\,\sigma_v^2\,\frac{1}{1\;+\;(\frac{1}{2}\;-\;4\,(\sin\phi)^2)\,|\bar{\beta}|^2}\,. \tag{28}$$

Based on the last expressions and neglecting the terms of order higher that 2, the likelihood function (25) becomes:

$$\Lambda(\phi,\bar{\beta}) \;\approx\; \Lambda_0(\phi) \;+\; \Lambda_r(\phi,\bar{\beta}_r) \;+\; \Lambda_i(\phi,\bar{\beta}_i) \tag{29}$$

with:

$$\Lambda_0(\phi) := -\frac{1}{4\sigma_v^2} b_0(\phi) \tag{30}$$

$$\Lambda_r(\phi,\bar{\beta}_r) := -\frac{1}{4\sigma_v^2}\left(b_{1r}(\phi)\bar{\beta}_r + (b_2(\phi) + a_2(\phi)b_0(\phi))\bar{\beta}_r^2\right) \tag{31}$$

$$\Lambda_i(\phi,\bar{\beta}_i) := -\frac{1}{4\sigma_v^2}\left(b_{1i}(\phi)\bar{\beta}_i + (b_2(\phi) + a_2(\phi)b_0(\phi))\bar{\beta}_i^2)\right) \tag{32}$$

in which $\bar{\beta}_r$ and $\bar{\beta}_i$ denote the real and imaginary parts of $\bar{\beta}$, and

$$a_2(\phi) \;:= \frac{1}{2} - 4(\sin\phi)^2 \tag{33}$$

$$b_0(\phi) \;:= (\underline{Z}_0^H\,\underline{Z}_0) + (\underline{Z}_1^H\,\underline{Z}_1) - 2\Re(\underline{Z}_1^H\,\underline{Z}_0)\cos\phi - 2\Im(\underline{Z}_1^H\,\underline{Z}_0)\sin\phi \tag{34}$$

$$b_{1r}(\phi) \;:= \;-\,4\Im(\underline{Z}_0^T\,\underline{Z}_1)\sin\phi - 4\Re(\underline{Z}_0^T\,\underline{Z}_0)(\sin\phi)^2 + 4\Im(\underline{Z}_0^T\,\underline{Z}_0)\sin\phi\cos\phi \tag{35}$$

$$b_{1i}(\phi) \;:= 4\Re(\underline{Z}_0^T\,\underline{Z}_1)\sin\phi - 4\Re(\underline{Z}_0^T\,\underline{Z}_0)\sin\phi\cos\phi - 4\Re(\underline{Z}_0^T\,\underline{Z}_0)(\sin\phi)^2 \tag{36}$$

$$b_2(\phi) \;:= 8(\underline{Z}_0^H\,\underline{Z}_0)(\sin\phi)^2 - 4\Im(\underline{Z}_1^H\,\underline{Z}_0)\sin\phi\,. \tag{37}$$

The term $a_2(\phi)$ is the term in $|\bar{\beta}|^2$ coming from the inverse of the noise variance in (25). The term $b_0(\phi)$ is the term independent of $\bar{\beta}$, the terms $b_{1r}(\phi)$ and $b_{1i}(\phi)$ are the terms in $\bar{\beta}_r$ and $\bar{\beta}_i$ and the term $b_2(\phi)$ is the term in $|\bar{\beta}|^2$ coming from the vector product in (25).

A usual approach to maximize the likelihood function over two parameters is to estimate iteratively the parameters after each other. The iterative EM algorithm is known to converge to the ML estimate.

IV. EM ALGORITHM

The EM algorithm is typically used to estimate a set of parameters based on a given observation when unknown random processes perturbate the observation. In our case, the phase ϕ due to the CFO is estimated based on the received vectors $\underline{Z}_0$ and $\underline{Z}_1$. The IQ imbalance $\bar{\beta}$ perturbates the estimation of ϕ.

Mathematically, one iteration of the EM algorithm is described as follows. If ϕ^i denotes the estimate of the phase ϕ at the iteration i, the estimate at the next iteration $i+1$ is given by [12]:

$$\phi^{i+1} \;=\; \max_{\phi} \int_{\bar{\beta}_r} \int_{\bar{\beta}_i} \Lambda(\phi, \bar{\beta})\, e^{\Lambda(\phi^i, \bar{\beta})}\, d\bar{\beta}_r\, d\bar{\beta}_i\,. \tag{38}$$

The phase selected at the new iteration is the one that maximizes the conditional expectation of the likelihood function over the IQ imbalance perturbation, given the most recent estimate of the phase.

Because the approximation (29) of the likelihood function (25) is decomposed into two independent functions (one depends on $\bar{\beta}_r$, the other depends on $\bar{\beta}_i$), it is also possible to simplify the double integral in (38) in two independent integrals. The expression (29) is equal to:

$$\begin{aligned} \phi^{i+1} \;=\; \max_{\phi} \big(&-b_0(\phi) - b_{1r}(\phi)\,\bar{\beta}_r^i - b_{1i}(\phi)\,\bar{\beta}_i^i \\ &- (b_2(\phi) + a_2(\phi) b_0(\phi))(\bar{\beta}_r^2)^i \\ &- (b_2(\phi) + a_2(\phi) b_0(\phi))(\bar{\beta}_i^2)^i) \end{aligned} \tag{39}$$

in which the following definitions have been made:

$$\bar{\beta}_r^i := \int_{\bar{\beta}_r} \bar{\beta}_r \, F_r(\bar{\beta}_r) \, d\bar{\beta}_r \tag{40}$$

$$\bar{\beta}_i^i := \int_{\bar{\beta}_i} \bar{\beta}_i \, F_i(\bar{\beta}_i) \, d\bar{\beta}_i \tag{41}$$

$$(\bar{\beta}_r^2)^i := \int_{\bar{\beta}_r} (\bar{\beta}_r^2) \, F_r(\bar{\beta}_r) \, d\bar{\beta}_r \tag{42}$$

$$(\bar{\beta}_i^2)^i := \int_{\bar{\beta}_i} (\bar{\beta}_i^2) \, F_i(\bar{\beta}_i) \, d\bar{\beta}_i \tag{43}$$

with:

$$F_r(\bar{\beta}_r) := \frac{e^{\Lambda_r(\phi^i, \bar{\beta}_r)}}{\int_{\bar{\beta}_r} e^{\Lambda_r(\phi^i, \bar{\beta}_r)} \, d\bar{\beta}_r} \tag{44}$$

$$F_i(\bar{\beta}_i) := \frac{e^{\Lambda_i(\phi^i, \bar{\beta}_i)}}{\int_{\bar{\beta}_i} e^{\Lambda_i(\phi^i, \bar{\beta}_i)} \, d\bar{\beta}_i} \, . \tag{45}$$

Interestingly, the function $F_r(\bar{\beta}_r)$ can be seen as the probability distribution of a Gaussian random variable of mean $-b_{1r}(\phi^i)/2(b_2(\phi^i) + a_2(\phi^i)b_0(\phi^i))$ and of variance $2\sigma_v^2/(b_2(\phi^i) + a_2(\phi^i)b_0(\phi^i))$. Equivalently, the function $F_i(\bar{\beta}_i)$ can be seen as the probability distribution of a Gaussian random variable of mean $-b_{1i}(\phi^i)/2(b_2(\phi^i) + a_2(\phi^i)b_0(\phi^i))$ and of variance $2\sigma_v^2/(b_2(\phi^i) + a_2(\phi^i)b_0(\phi^i))$. Therefore, we obtain:

$$\bar{\beta}_r^i = -\frac{b_{1r}(\phi^i)}{2(b_2(\phi^i) + a_2(\phi^i)b_0(\phi^i))} \tag{46}$$

$$\bar{\beta}_i^i = -\frac{b_{1i}(\phi^i)}{2(b_2(\phi^i) + a_2(\phi^i)b_0(\phi^i))} \tag{47}$$

$$(\bar{\beta}_r^2)^i = \frac{2\sigma_v^2}{(b_2(\phi^i) + a_2(\phi^i)b_0(\phi^i))} + (\bar{\beta}_r^i)^2 \tag{48}$$

$$(\bar{\beta}_i^2)^i = \frac{2\sigma_v^2}{(b_2(\phi^i) + a_2(\phi^i)b_0(\phi^i))} + (\bar{\beta}_i^i)^2 \, . \tag{49}$$

The two last equalities have been obtained because the auto-correlation is equal to the variance plus the square of the mean. It is interesting to note that the expressions (46) and (47) correspond to the ML estimate of the parameters $\bar{\beta}_r$ and $\bar{\beta}_i$ for a given phase ϕ equal to ϕ^i (the mean of a Gaussian variable is also the value that maximizes the distribution). The estimate of the square of the parameters $\bar{\beta}_r$ and $\bar{\beta}_i$ given in (48) and (49) is however equal to the square of the ML estimates plus a correction term.

The EM iterative algorithm can be summarized as follows:

1. Start from an initial estimate of the phase ϕ^0,
2. At the iteration i, evaluate the parameters $a_2(\phi^i)$, $b_0(\phi^i)$, $b_{1r}(\phi^i)$, $b_{1i}(\phi^i)$ and $b_2(\phi^i)$ according to the definitions (33)-(37) based on the value ϕ^i,
3. Estimate the real part $\bar{\beta}_r^i$ and the imaginary part $\bar{\beta}_i^i$ of the IQ imbalance, and their square $(\bar{\beta}_r^2)^i$ and $(\bar{\beta}_i^2)^i$ according to the results (46)-(49),
4. Select the phase ϕ^{i+1} such that the function (39) is maximized,
5. Iterate on the steps 2 to 4, until the algorithm converges.

The initial phase estimate is typically obtained by neglecting the IQ imbalance and by using the algorithm proposed by Schmidl and Cox [6].

V. IMPLEMENTATION

The critical part of the computational effort resides in the search of the value ϕ^{i+1} that maximizes the function (39) at each iteration (step 4 in the previous section). Obviously, the parameters (33)-(37) and the function (39) can be computed for all possible values of ϕ, and the optimal value ϕ^{i+1} can be selected. In this section, we simplify rather the search of the maximum based on trigonometric identities and based on the method of Newton-Raphson to find the roots of a function.

Assuming that the sine and cosine functions are implemented with a lookup table, it is interesting to apply the following trigonometric identities in order to avoid the multiplications:

$$(\sin\phi)^2 = \frac{1}{2} - \frac{1}{2}\cos(2\phi) \tag{50}$$

$$\sin\phi\cos\phi = \frac{1}{2}\sin(2\phi) \tag{51}$$

$$(\sin\phi)^3 = \frac{3}{4}\sin\phi - \frac{1}{4}\sin(3\phi) \tag{52}$$

$$(\sin\phi)^2\cos\phi = \frac{1}{4}\cos\phi - \frac{1}{4}\cos(3\phi)\,. \tag{53}$$

The equalities (33)-(37) can be easily modified according to (50)-(53) and included in the expression (39) of the phase estimate. It gives:

$$\phi^{i+1} = \max_{\phi} G(\phi) \tag{54}$$

with:

$$\begin{aligned} G(\phi) \;:=& \, p_1(\bar{\beta}^i)\,\cos\phi \;+\; q_1(\bar{\beta}^i)\,\sin\phi \\ &+\; p_2(\bar{\beta}^i)\,\cos(2\phi) \;+\; q_2(\bar{\beta}^i)\,\sin(2\phi) \\ &+\; p_3(\bar{\beta}^i)\,\cos(3\phi) \;+\; q_3(\bar{\beta}^i)\,\sin(3\phi) \end{aligned} \tag{55}$$

in which $\bar{\beta}^i$ denotes the set of parameters $\left\{\bar{\beta}_r^i, \bar{\beta}_i^i, (\bar{\beta}_r^2)^i, (\bar{\beta}_i^2)^i\right\}$, and:

$$p_1(\bar{\beta}^i) \;:= \Re(\underline{Z}_1^H\,\underline{Z}_0)\,\left(2-(\bar{\beta}_r^2)^i-(\bar{\beta}_i^2)^i\right) \tag{56}$$

$$\begin{aligned} q_1(\bar{\beta}^i) \;:=& \, \Im(\underline{Z}_1^H\,\underline{Z}_0)\,\left(2-(\bar{\beta}_r^2)^i-(\bar{\beta}_i^2)^i\right) \\ &+\; 4\,\left(\Im(\underline{Z}_0^T\,\underline{Z}_1)\,\bar{\beta}_r^i - \Re(\underline{Z}_0^T\,\underline{Z}_1)\,\bar{\beta}_i^i\right) \end{aligned} \tag{57}$$

$$\begin{aligned} p_2(\bar{\beta}^i) \;:=& \; -\,2\,\left(\Re(\underline{Z}_0^T\,\underline{Z}_0)\,\bar{\beta}_r^i + \Im(\underline{Z}_0^T\,\underline{Z}_0)\,\bar{\beta}_i^i\right) \\ &+\; 2\,\left((\bar{\beta}_r^2)^i+(\bar{\beta}_i^2)^i\right)\,\left((\underline{Z}_0^H\,\underline{Z}_0)-(\underline{Z}_1^H\,\underline{Z}_1)\right) \end{aligned} \tag{58}$$

$$q_2(\bar{\beta}^i) \;:=\; -\,2\,\left(\Im(\underline{Z}_0^T\,\underline{Z}_0)\,\bar{\beta}_r^i - \Re(\underline{Z}_0^T\,\underline{Z}_0)\,\bar{\beta}_i^i\right) \tag{59}$$

$$p_3(\bar{\beta}^i) \;:= 2\,\Re(\underline{Z}_1^H\,\underline{Z}_0)\,\left((\bar{\beta}_r^2)^i+(\bar{\beta}_i^2)^i\right) \tag{60}$$

$$q_3(\bar{\beta}^i) \;:= 2\,\Im(\underline{Z}_1^H\,\underline{Z}_0)\,\left((\bar{\beta}_r^2)^i+(\bar{\beta}_i^2)^i\right)\,. \tag{61}$$

Finding the maximum in (55) is equivalent to finding the root of the first order derivative $G'(\phi)$ of the function $G(\phi)$. It gives:

$$G'(\phi^{i+1}) \;=\; 0 \tag{62}$$

with:

$$\begin{aligned} G'(\phi) \;:=& \; -\,p_1(\bar{\beta}^i)\,\sin\phi \;+\; q_1(\bar{\beta}^i)\,\cos\phi \\ &-\; 2p_2(\bar{\beta}^i)\,\sin(2\phi) \;+\; 2q_2(\bar{\beta}^i)\,\cos(2\phi) \\ &-\; 3p_3(\bar{\beta}^i)\,\sin(3\phi) \;+\; 3q_3(\bar{\beta}^i)\,\cos(3\phi)\,. \end{aligned} \tag{63}$$

We propose to apply the iterative method of Newton-Raphson to evaluate the roots of a function (see Figure 2). The new value is given by the zero of the tangent of the function at the current value. At the iteration n, the new estimate of the root is given by:

$$\phi^{i+1}(n+1) \;=\; \phi^{i+1}(n) \;-\; \frac{G'(\phi^{i+1}(n))}{G''(\phi^{i+1}(n))} \tag{64}$$

in which $G''(\phi^{i+1}(n))$ denotes the second order derivative of $G(\phi)$. In order to have a reliable initial estimate, it is useful to remark that the terms in $p_1(\bar{\beta}^i)$ and $q_1(\bar{\beta}^i)$ in (63) are dominant. A good starting point is therefore:

$$\phi^{i+1}(0) = \begin{cases} \arctan\left(\frac{q_1(\bar{\beta}^i)}{p_1(\bar{\beta}^i)}\right) & \text{if } p_1 \geq 0 \\ \arctan\left(\frac{q_1(\bar{\beta}^i)}{p_1(\bar{\beta}^i)}\right) + \pi & \text{if } p_1 < 0, q_1 \geq 0 \\ \arctan\left(\frac{q_1(\bar{\beta}^i)}{p_1(\bar{\beta}^i)}\right) - \pi & \text{if } p_1 < 0, q_1 < 0 \end{cases} \tag{65}$$

because $\phi^{i+1}(0)$ is a root of the function $G'(\phi)$ corresponding to a maximum of the function $G(\phi)$ (and not to a minimum) if the terms $p_2(\bar{\beta}^i)$, $q_2(\bar{\beta}^i)$, $p_3(\bar{\beta}^i)$ and $q_3(\bar{\beta}^i)$ are negligible.

VI. RESULTS

The goal of the present section is to assess the performance of the EM algorithm and to compare it to the performance of the initial algorithm proposed by Schmidl and Cox [6] and to the performance of the ML estimator. As an example, we consider a typical WLAN system. The system operates in an indoor environment at 5 GHz with a 20 MHz bandwidth. According to the IEEE 802.11a standard, each transmitted burst consists of a preamble followed by regular OFDM symbols. The first 4 μs of the preamble are used for automatic gain control (AGC). The next 4 μs of the preamble can be used for packet detection, and coarse timing/frequency synchronization. The last 8 μs of the preamble are used for synchronization refinement and channel estimation. We focus on the last part of the preamble dedicated to the fine synchronization and composed of a cyclic prefix of length 32, followed by a sequence of length 64 (the C sequence) repeated one time. The propagation environment is modeled by the static HiperLAN2 type A channel model, which is characterized by a smoothly decreasing power/delay profile with a maximum excess delay of 390 ns. The performance is averaged over 1000 channel realizations.

The standard deviation of the estimated frequency error and of the estimated IQ imbalance error is illustrated in Figures 3 and 4 respectively for the different estimation schemes as a function of the SNR. We assume a fixed value of the CFO equal to 50 kHz ($\phi = 2$) and a fixed value of the IQ imbalance equal to 10 % ($\bar{\beta} = 0.1e^{j3\pi/8}$). The initial CFO estimate (Schmidl and Cox) has a performance near to the one of the ML algorithm at low SNR and floors to a poor estimate at high SNR because it does not take the IQ imbalance into account. Starting from this initial estimate, the EM algorithm converges progressively to the ML estimate and

outperforms significantly the initial CFO estimate. Less than 3 iterations are needed to reach the point of convergence. At low SNR (less than 10 dB), the EM algorithm suffers however from the fact that we have neglected the first term in (25) to obtain the approximated likelihood function (29). At high SNR (more than 35 dB), the EM algorithm suffers also from the second order approximation in the IQ imbalance performed to obtain the approximated likelihood function (29). Comparing the Figures 3 and 4, it is clear that mostly the EM estimate of the IQ imbalance suffers from the two approximations while the EM estimate of the CFO is quite robust.

Figure 5 illustrates the standard deviation of the frequency estimation error (solid curves) and of the IQ imbalance estimation error (dashed curves) as a function of the IQ imbalance for an SNR equal to 20 dB. The performance of the initial frequency estimator degrades fast with the value of the IQ imbalance, while the performance of the EM algorithm remains close to the one of the ML algorithm. Interestingly, the EM frequency and IQ imbalance estimator performance is nearly independent from the value of the IQ imbalance.

Figure 6 illustrates the standard deviation of the frequency estimation error (solid curves) and of the IQ imbalance estimation error (dashed curves) as a function of the CFO for an SNR equal to 20 dB. The performance of the EM algorithm remains close to the one of the ML algorithm. The quality of the CFO estimate varies slightly as a function of the CFO (except on the borders of the range where there is a phase ambiguity between $+\pi$ and $-\pi$). On the other hand, the quality of the IQ imbalance estimate is strongly dependent on the CFO. When $\phi = 0$ (CFO $= 0$) or when $\phi = \pm\pi$ (CF0 $= \pm 150$kHz), the two vectors $\underline{Z}_0$ and $\underline{Z}_1$ in the model (16)-(17) become identical (except for the contribution of the noise). It is therefore impossible to discriminate between the two unknown parameters $\bar{\beta}$ and $\underline{X}$ based on the observation of $\underline{Z}_0$ and $\underline{Z}_1$. In order to solve this problem, an artificial CFO can be added on the same preamble sent a second time [11]. Another solution would be to estimate the IQ imbalance later in the receiver. Typically the IQ imbalance can also be well estimated together with the channel [13].

VII. CONCLUSION

This paper addresses the problem of the joint estimation of the CFO, generated by the local oscillators, and of the IQ imbalance, present when direct-conversion radio frequency transceivers are used. A low-complexity iterative solution, based on the EM algorithm, has been designed. The solution makes use of a repetitive preamble so that the knowledge of the propagation channel

is not required. A second order approximation of the likelihood function has been made and the expressions have been simplified into an implementable form. The EM estimate of the CFO is shown to converge to the ML estimate on all the SNR/CFO/IQ imbalance range. However, the EM estimate of the IQ imbalance is more sensitive to the different parameters. The accuracy of the IQ imbalance estimate is especially reduced at low and high SNR values, because the approximation of the likelihood function is not correct anymore, and at low CFO values, because the initial model lacks of information in this case. Less than 3 iterations are required to reach the point of convergence.

APPENDIX

The goal of this appendix is to compute the variance of the noise vector in (19). The noise vector is defined as:

$$\underline{N} \,:=\, -\lambda(\phi,\bar{\beta})\,\underline{V}_0 \,-\, \mu(\phi,\bar{\beta})\,\underline{V}_0^* \,+\, \underline{V}_1 \tag{66}$$

in which the vectors $\underline{V}_0$ and $\underline{V}_1$ are composed of Q Gaussian independent elements of zero mean and of variance σ_v^2. Let $\underline{V}_0^R$ and $\underline{V}_0^I$ denote the real and imaginary parts of $\underline{V}_0$, $\underline{V}_1^R$ and $\underline{V}_1^I$ denote the real and imaginary parts of $\underline{V}_1$, and $\bar{\beta}^R$ and $\bar{\beta}^I$ denote the real and imaginary parts of $\bar{\beta}$. By taking the definitions (20) and (21) of the functions $\lambda(\phi,\bar{\beta})$ and $\mu(\phi,\bar{\beta})$ into account, the vector $\underline{N}$ is equal to:

$$\begin{aligned}\underline{N} \,=\, & \underline{V}_0^R \left[\left(-\cos\phi \,+\, 2\,\sin\phi\,\frac{\bar{\beta}^I}{1\,-\,|\bar{\beta}|^2}\right) \,+\, j\,\left(\sin\phi\,\frac{1\,+\,|\bar{\beta}|^2}{1\,-\,|\bar{\beta}|^2} \,-\, 2\,\sin\phi\,\frac{\bar{\beta}^R}{1\,-\,|\bar{\beta}|^2}\right)\right] \\ & +\, \underline{V}_0^I \left[j\,\left(-\cos\phi \,-\, 2\,\sin\phi\,\frac{\bar{\beta}^I}{1\,-\,|\bar{\beta}|^2}\right) \,+\, \left(-\sin\phi\,\frac{1\,+\,|\bar{\beta}|^2}{1\,-\,|\bar{\beta}|^2} \,-\, 2\,\sin\phi\,\frac{\bar{\beta}^R}{1\,-\,|\bar{\beta}|^2}\right)\right] \\ & +\, \underline{V}_1^R \,+\, j\,\underline{V}_1^I\,.\end{aligned} \tag{67}$$

The variance of the real part $\underline{N}^R$ of $\underline{N}$ is equal to

$$\begin{aligned}\sigma_{n^R}^2(\phi,\bar{\beta}) \,=\, & \sigma_{v_0^R}^2\,\frac{1}{(1\,-\,|\bar{\beta}|^2)^2}\,\left(\cos\phi\,(1\,-\,|\bar{\beta}|^2) \,-\, 2\,\sin\phi\,\bar{\beta}^I\right)^2 \\ & +\, \sigma_{v_0^I}^2\,\frac{1}{(1\,-\,|\bar{\beta}|^2)^2}\,\left(\sin\phi\,(1\,+\,|\bar{\beta}|^2) \,+\, 2\,\sin\phi\,\bar{\beta}^R\right)^2 \,+\, \sigma_{v_1^R}^2\end{aligned} \tag{68}$$

and the variance of the imaginary part $\underline{N}^I$ of $\underline{N}$ is equal to

$$\begin{aligned}\sigma_{n^I}^2(\phi,\bar{\beta}) \,=\, & \sigma_{v_0^R}^2\,\frac{1}{(1\,-\,|\bar{\beta}|^2)^2}\,\left(\sin\phi\,(1\,+\,|\bar{\beta}|^2) \,-\, 2\,\sin\phi\,\bar{\beta}^R\right)^2 \\ & +\, \sigma_{v_0^I}^2\,\frac{1}{(1\,-\,|\bar{\beta}|^2)^2}\,\left(\cos\phi\,(1\,-\,|\bar{\beta}|^2) \,+\, 2\,\sin\phi\,\bar{\beta}^I\right)^2 \,+\, \sigma_{v_1^I}^2\end{aligned} \tag{69}$$

in which $\sigma^2_{v_0^R}$, $\sigma^2_{v_0^I}$, $\sigma^2_{v_1^R}$, $\sigma^2_{v_1^I}$ are the variances of the real and imaginary parts of the vectors $\underline{V}_0$ and $\underline{V}_1$ respectively, equal to $\sigma_v^2/2$. By adding the two terms (real and imaginary parts), the total variance of the elements of the noise $\underline{N}$ is equal to:

$$\begin{aligned}\sigma_n^2(\phi,\bar{\beta}) &= \sigma_{n^R}^2(\phi,\bar{\beta}) + \sigma_{n^I}^2(\phi,\bar{\beta}) \\ &= \sigma_v^2\left(2 - |\bar{\beta}|^2 + 8\left(\sin\phi\right)^2 \frac{|\bar{\beta}|^2}{1 - |\bar{\beta}|^2}\right)\end{aligned} \tag{70}$$

which is the result given in (23).

REFERENCES

[1] R. van Nee, G. Awater, M. Morikura, H. Takanashi, M. Webster, and K.W. Halford, "New high-rate wireless LAN standards," *IEEE Communications Magazine*, vol. 37, no. 12, pp. 82–88, December 1999.

[2] "3GPP TR 25.814, 3rd generation partnership project; technical specification group radio access network; physical layer aspects for evolved UTRA," http://www.3gpp.org.

[3] A. A. Abidi, "Direct-conversion radio transceivers for digital communications," *IEEE Journal on Solid-State Circuits*, vol. 30, no. 12, pp. 1399–1410, December 1995.

[4] F. Horlin, S. De Rore, E. Lopez-Estraviz, F. Naessens, and L. Van der Perre, "Impact of frequency offsets and IQ imbalance on MC-CDMA reception based on channel tracking," *IEEE Journal on Selected Areas in Communications*, vol. 24, no. 6, June 2006.

[5] A. Tarighat, R. Bagheri, and A. H. Sayed, "Compensation schemes and performance analysis of IQ imbalances in OFDM receivers," *IEEE Transactions on Signal Processing*, vol. 53, no. 8, pp. 3257–3268, August 2005.

[6] T. M. Schmidl and D. C. Cox, "Robust frequency and timing synchronization for OFDM," *IEEE Transactions on Communications*, vol. 45, no. 12, pp. 1613–1621, December 1997.

[7] S. Fouladifard and H. Shafiee, "Frequency offset estimation in OFDM systems in presence of IQ imbalance," in *IEEE Proceedings of ICC*, May 2003, vol. 3, pp. 2071–2075.

[8] F. Yan, W-P. Zhu, and M. Omair Ahmad, "Carrier frequency offset estimation for OFDM systems with I/Q imbalance," in *IEEE Proceedings of 47th International Midwest Symposium on Circuits and Systems*, July 2004, vol. 2, pp. 633–636.

[9] J. Tubbax, B. Come, L. Van der Perre, S. Donnay, M. Engels, M. Moonen, and H. De Man, "Joint compensation of IQ imbalance and frequency offset in OFDM systems," in *IEEE Proceedings of Radio Wireless Conference*, August 2003, pp. 39–42.

[10] G. Xing, M. Shen, and H. Liu, "Frequency offset and I/Q imbalance compensation for direct-conversion receivers," *IEEE Transactions on Wireless Communications*, vol. 4, no. 2, pp. 673–680, March 2005.

[11] S. De Rore, E. Lopez-Estraviz, F. Horlin, and L. Van der Perre, "Joint estimation of carrier frequency offset and IQ imbalance for 4G mobile wireless systems," in *Proceedings of ICC*, June 2006.

[12] T. K. Moon, "The expectation maximization algorithm," *IEEE Signal Processing Magazine*, vol. 13, no. 6, pp. 47–59, November 1996.

[13] E. Lopez-Estraviz, S. De Rore, , F. Horlin, and L. Van der Perre, "Optimal training sequences for joint channel and frequency-dependent iq imbalance estimation in ofdm-based receivers," in *Proceedings of ICC*, June 2006.

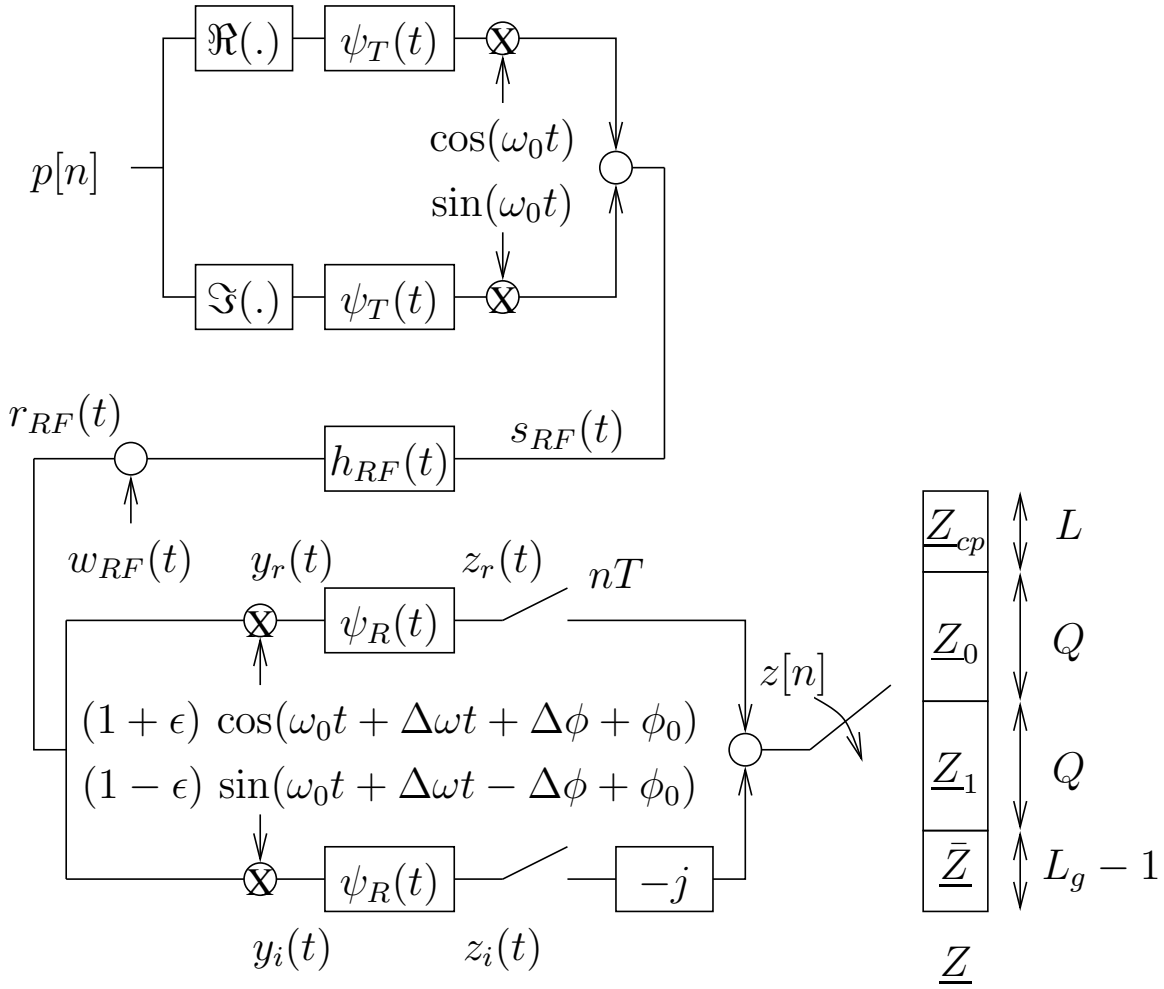

Fig. 1. System model.

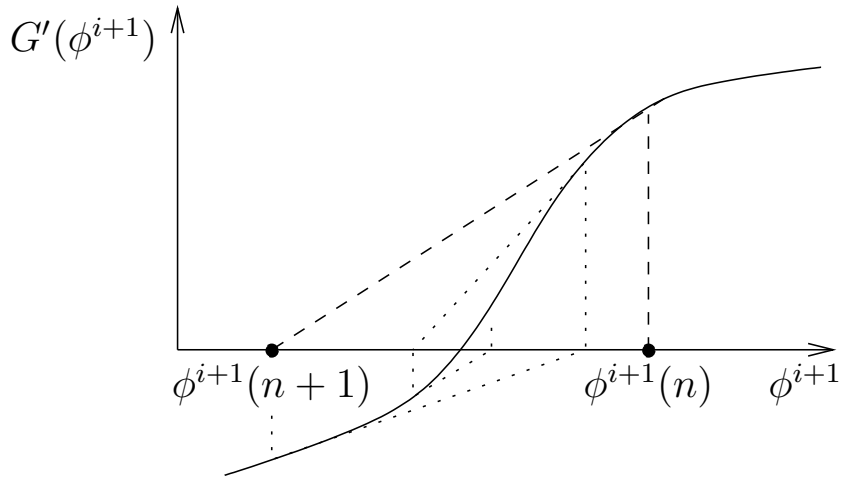

Fig. 2. Newton Raphson.

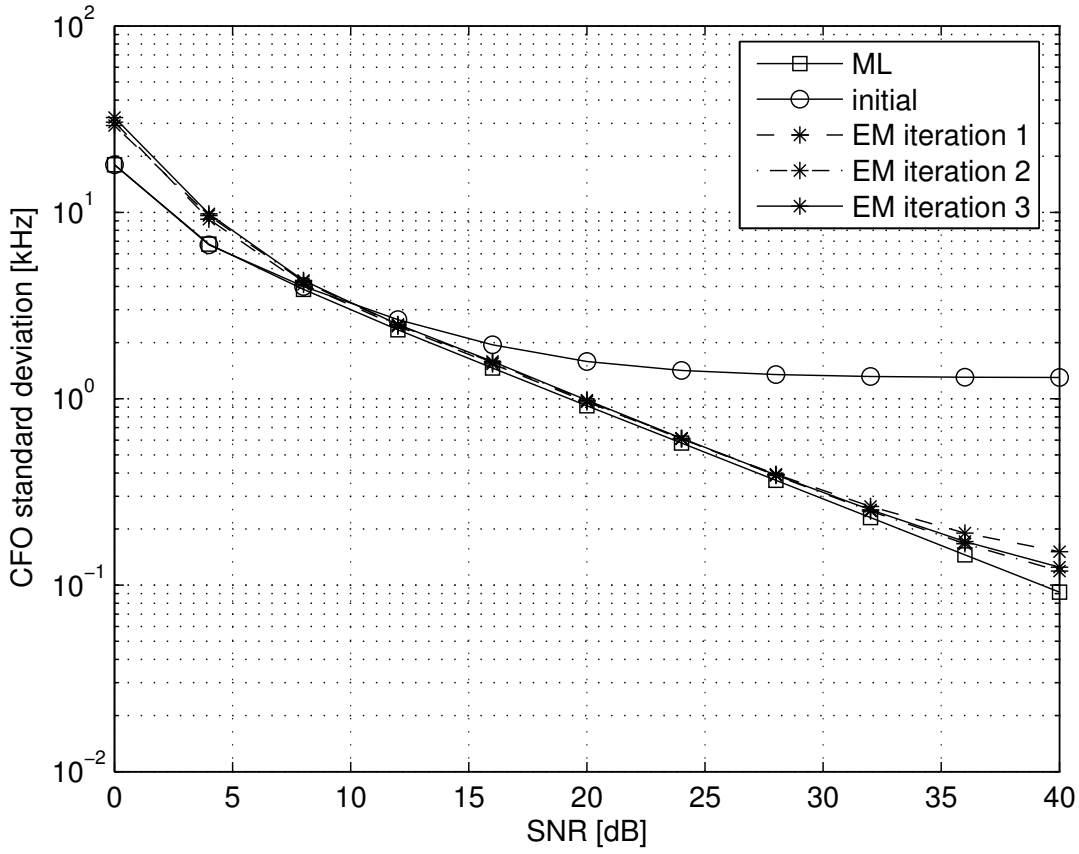

Fig. 3. Frequency estimate error standard deviation as a function of the SNR, $\phi = 2$, $\bar{\beta} = 0.1e^{j3\pi/8}$.

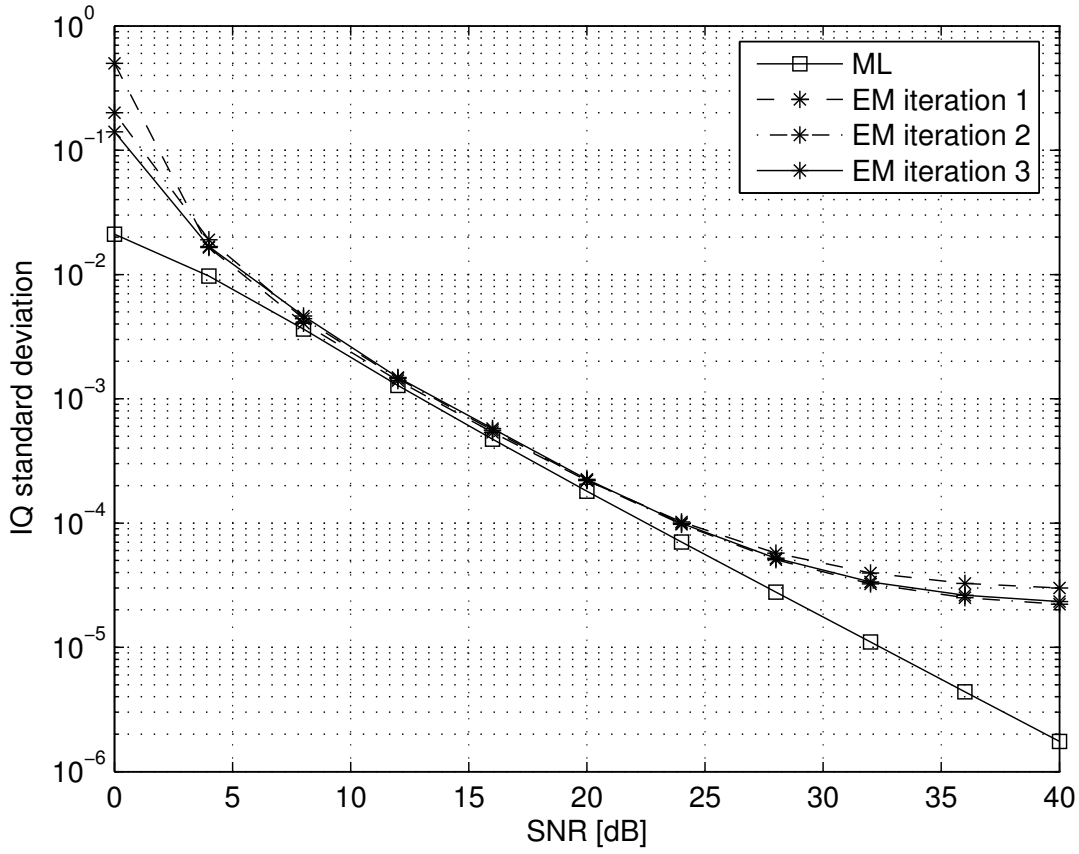

Fig. 4. IQ imbalance estimation error standard deviation as a function of the SNR, $\phi = 2$, $\bar{\beta} = 0.1e^{j3\pi/8}$.

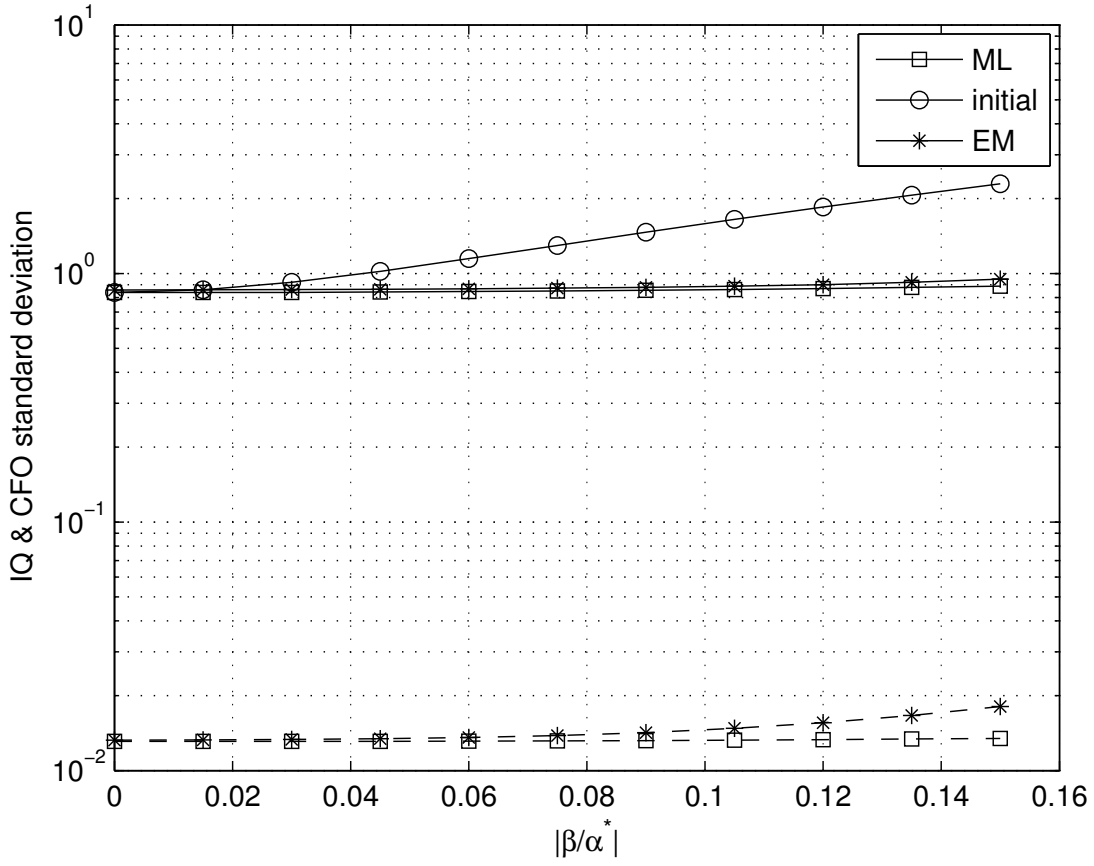

Fig. 5. Solid curves: frequency estimate error standard deviation, dashed curves: IQ imbalance estimate error standard deviation, $\phi = 2$, $\angle\bar{\beta} = 3\pi/8$, SNR $= 20$ dB.

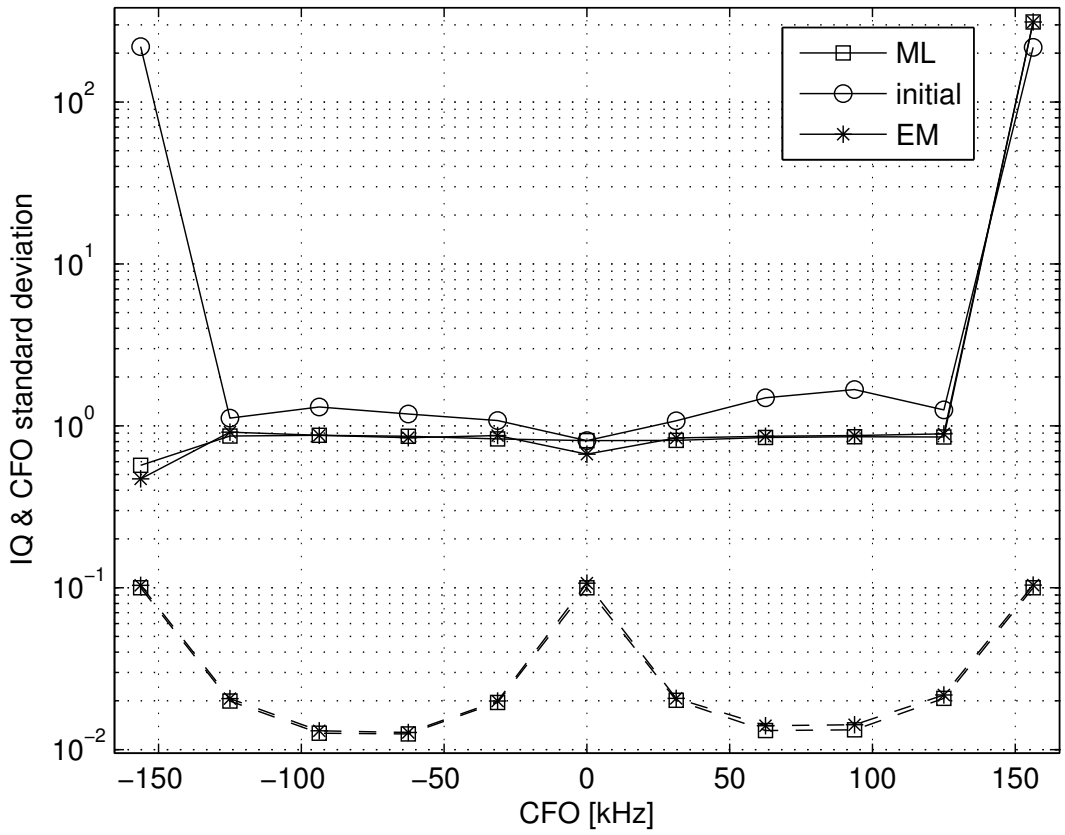

Fig. 6. Solid curves: frequency estimate error standard deviation, dashed curves: IQ imbalance estimate error standard deviation, $\bar{\beta} = 0.1e^{j3\pi/8}$, SNR $= 20$ dB.